AFRL-ML-TY-TR-2002-4547

Dense Non-Aqueous Phase Liquid (DNAPL) Physical Modeling Study

Mark Newman
University of Florida

Gainesville, FL 32611

Joel S. Hayworth
Applied Research Associates, Inc.
215 Harrison Ave
Panama City, FL 32401

Thomas B. Stauffer
Air Force Research Laboratory
139 Barnes Drive Suite 2
Tyndall AFB FL 32403-5323

AIR FORCE RESEARCH LABORATORY
MATERIALS & MANUFACTURING DIRECTORATE
AIR EXPEDITIONARY FORCES TECHNOLOGIES DIVISION
139 BARNES DRIVE, STE 2
TYNDALL AFB FL 32403-5323

20020830 019

NOTICES

USING GOVERNMENT DRAWINGS, SPECIFICATIONS, OR OTHER DATA INCLUDED IN THIS DOCUMENT FOR ANY PURPOSE OTHER THAN GOVERNMENT PROCUREMENT DOES NOT IN ANY WAY OBLIGATE THE US GOVERNMENT. THE FACT THAT THE GOVERNMENT FORMULATED OR SUPPLIED THE DRAWINGS, SPECIFICATIONS, OR OTHER DATA DOES NOT LICENSE THE HOLDER OR ANY OTHER PERSON OR CORPORATION; OR CONVEY ANY RIGHTS OR PERMISSION TO MANUFACTURE, USE, OR SELL ANY PATENTED INVENTION THAT MAY RELATE TO THEM.

THIS REPORT IS RELEASABLE TO THE NATIONAL TECHNICAL INFORMATION SERVICE
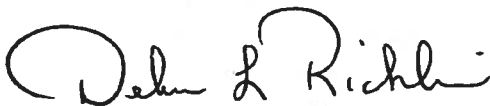5285 PORT ROYAL RD.
SPRINGFIELD VA 22 161
TELEPHONE 703 487 4650; 703 4874639 (TDD for the hearing-impaired)
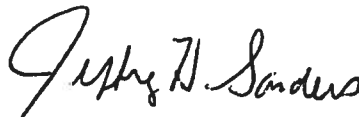E-MAIL   orders@ntis.fedworld.gov
WWW   http://www.ntis.gov/index.html

AT NTIS, IT WILL BE AVAILABLE TO THE GENERAL PUBLIC, INCLUDING FOREIGN NATIONS.

THIS TECHNICAL REPORT HAS BEEN REVIEWED AND IS APPROVED FOR PUBLICATION.

DEBRA L. RICHLIN, MAJ USAF
Program Manager

JEFFERY H. SANDERS
Chief, Weapons Systems Logistics Branch

DONALD R. HUCKLE, JR., Colonel, USAF
Chief, Air Expeditionary Forces Technologies Division

Do not return copies of this report unless contractual obligations or notice on a specific document requires its return.

REPORT DOCUMENTATION PAGE

Form Approved
OMB No. 0704-0188

1. AGENCY USE ONLY *(Leave blank)*	2. REPORT DATE July 2002	3. REPORT TYPE AND DATES COVERED 1 Oct 1995 – 30 Sept 1997	

4. TITLE AND SUBTITLE Dense Non-Aqueous Phase Liquid (DNAPL) Physical Modeling Study	5. FUNDING NUMBERS JON: 1900B76A PE: 62202F
6. AUTHORS Newman, Mark, Hayworth, Joel S., Stauffer, Thomas B.	

7. PERFORMING ORGANIZATION NAME(S) AND ADDRESS(ES) Air Force Research Laboratory, Air Expeditionary Forces Technologies Division (AFRL/MLQ) 139 Barnes Drive, Suite 2	8. PERFORMING ORGANIZATION REPORT NUMBER

9. SPONSORING/MONITORING AGENCY NAME(S) AND ADDRESS(ES) Air Force Research Laboratory, Air Expeditionary Forces Technologies Division (AFRL/MLQ) 139 Barnes Drive, Suite 2	10. SPONSORING/MONITORING AGENCY REPORT NUMBER AFRL-ML-TY-TR-2002-4547

11. SUPPLEMENTARY NOTES

12a. DISTRIBUTION/AVAILABILITY STATEMENT Distribution Unlimited; Approved for Public Release	12b. DISTRIBUTION CODE A

13. ABSTRACT *(Maximum 200 words)*

This document presents the results of a physical modeling study performed at the Air Force Research Laboratory (AFRL) between June 6, 1996 and September 6, 1997 by a multidisciplinary team comprised of University of Florida (UF), Applied Research Associates, Inc. (ARA), and AFRL researchers. This study investigated the dissolution behavior of dense non-aqueous phase liquids (DNAPLs) in threee-dimensional flow systems under controlled laboratory conditions.

14. SUBJECT TERMS Dense, Non-Aqueous, DNAPL	15. NUMBER OF PAGES 39
	16. PRICE CODE

17. SECURITY CLASSIFICATION OF REPORT UNCLASSIFIED	18. SECURITY CLASSIFICATION OF THIS PAGE UNCLASSIFIED	19. SECURITY CLASSIFICATION OF ABSTRACT UNCLASSIFIED	20. LIMITATION OF ABSTRACT UL

NSN 7540-01-280-5500   Computer Generated   STANDARD FORM 298 (Rev 2-89)
Prescribed by ANSI Std 239-18
298-102

i

TABLE OF CONTENTS

LIST OF TABLES

LIST OF FIGURES

EXECUTIVE SUMMARY

This document presents the results of a physical modeling study performed at the Air Force Research Laboratory (AFRL) between June 6, 1996 and September 6, 19x97 by a multi-disciplinary team comprised of AFRL, University of Florida (UF), Applied Research Associates, Inc. (ARA), and AFRL researchers. The overall purpose of the study was to investigate the dissolution behavior of dense nonaqueous phase liquids (DNAPLs) in three-dimensional flow systems under controlled laboratory conditions. Specific research objectives included:

1. Design and construct a physical modeling system for the purpose of conducting mass-conserving flow and transport experiments using chlorinated solvents.

2. Fully characterize flow hydraulics and transport hydrodynamics within the physical model

3. Perform chlorinated solvent dissolution experiments in homogeneous media to develop methods for source zone delineation

4. Perform chlorinated solvent dissolution experiments in heterogeneous media to expand source zone delineation methods

5. Examine partitioning and interfacial tracer methods under controlled laboratory conditions

During the course of this research project, objectives 1 through 3 were completed successfully. Early preparations for objectives 4 and 5 were begun but were halted due to program changes at AFRL. This report summarizes the work associated with objectives 1-3. The results of this study were utilized by the University of Florida to examine numerical modeling methods for source zone delineation; the reader is referred to the dissertation of Dr. Mark A. Newman for details.

INTRODUCTION

The validity of any contamination risk assessment depends upon adequate characterization of the contaminant source and the aquifer hydrogeological properties. Unfortunately, most field investigations leave subsurface sources poorly defined. This is especially true when the source contains dense nonaqueous phase liquids (DNAPLs) such as single or mixed chlorinated solvents. These compounds have very low water solubilities and therefore can serve as groundwater contaminants for decades or longer. Lack of resources and physical limitations on the standard intrusive methods for characterizing contaminant sources such as soil coring and cone penetrometer methods are the main reasons these source areas are often poorly defined. The development of technologies such as partitioning tracers and interfacial tracers offer in situ characterization alternatives to the traditional intrusive techniques (Jin et al., 1995; Annable et al., 1998a, b). However, application of in situ tracer techniques still require some general knowledge of the contaminant source location and distribution.

The purpose of the study documented in this report was to use physical modeling techniques to investigate the dissolution of multiple chlorinated solvent source zones in three-dimensional flow systems. As part of this study, techniques for locating and estimating the spatial distribution of DNAPL source areas were investigated. The results of an inverse modeling study using data generated during this study can be found in Newman (2001).

Physical models are simplified versions of the real system that are functional and provide the opportunity to perform physical experiments in order to simulate the responses of the system to applied conditions and stresses. There is typically a scale difference between the physical model and the real system; this must be considered in the simplifying assumptions and when analyzing the experimental results.

1

A conceptual model of a multi-source DNAPL zone is illustrated in Figure 1. For this conceptual model, the system of interest is an unconfined homogeneous sand aquifer in which all transport is taking place within the saturated zone. It is assumed that a zone of water-soluble contaminant has been introduced to the aquifer and that the contaminant is being transported in the direction of the natural groundwater gradient. The groundwater flow is assumed uniform and steady. It is also assumed that contaminant concentrations can be measured at multiple locations down gradient of the contaminant source zone. A flux plane is established so that it is perpendicular to the direction of groundwater flow. The conceptual model presented in Figure 1 was used to develop the physical model designed and constructed during this study, and forms the basis for the inverse source zone modeling performed by Newman (2001).
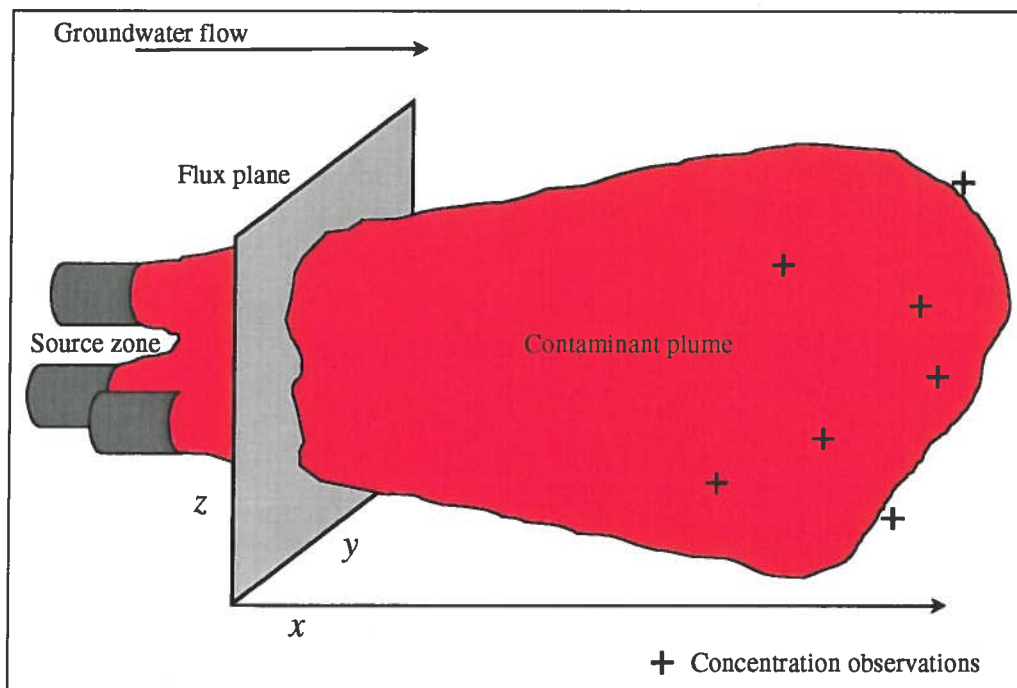
Figure 1. Conceptual model of multi-source DNAPL zone.

2

THREE-DIMENSIONAL PHYSICAL MODEL

Three-dimensional physical modeling provides a means to examine complex processes under controlled laboratory conditions. A particular strength of physical modeling is the ability to reproduce experiments; this allows systematic variation in experimental parameters not possible during field experiments. The ability to reproduce experimental conditions also allows verification of experimental results. The physical experiments in this study were designed to provide a sequential set of data to test the capabilities of the mathematical model and solution techniques presented in Newman (2001).

The aquifer model used in this study was constructed at the Air Force Research Laboratory, Tyndall Air Force Base, Florida (Figures 2 and 3). The system was designed for use with chlorinated solvents; all wetted surfaces are stainless steel or glass, minimizing the partitioning of hydrophobic chemicals to system components. All liquid effluent and vapor streams passed through physical and/or chemical traps, eliminating exposure to hazardous chemicals and allowing quantitative mass balance determinations. In the experiments performed for this study, the model was configured to simulate a homogeneous surficial aquifer. The porous medium was a clean, medium grained silica sand (Flint Silica #14).

The volumetric flowrate and corresponding pore water velocity were controlled by manipulating the elevations of the inlet and outlet head tanks. The physical, hydrodynamic, and transport characteristics of the system are presented in Table 1. The methods for determining these values are discussed in the following sections.

Figure 2. Front view of three-dimensional aquifer model (Air Force Research Laboratory, Tyndall Air Force Base, Florida)

Figure 3. Rear (sampling side) of three-dimensional aquifer model (Air Force Research Laboratory, Tyndall Air Force Base, Florida)

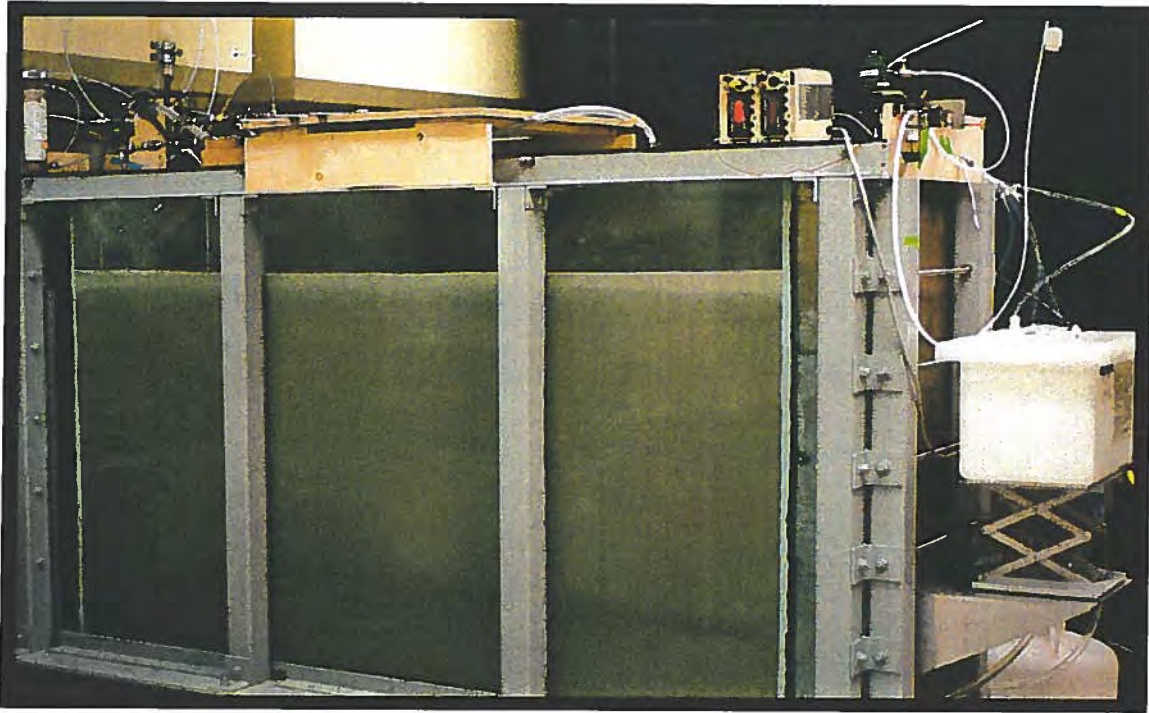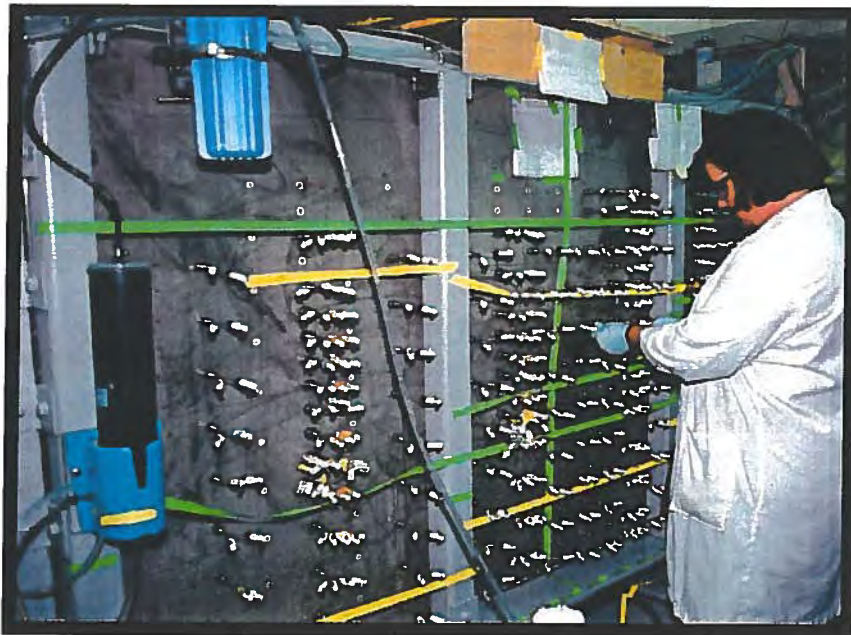<u>Multi-Point Samplers.</u> A series of multi-point samplers were emplaced within the flow system providing a three-dimensional distribution of over 500 sampling points within the porous media. The longitudinal distribution (x-z plane) of multi-point samplers is shown in Figure 4. The lateral distribution (y-z plane) of sample points varies with location along the longitudinal (x) axis. Some transects have a minimum of 20 sample points while the more extensive transects have up to 72 sample points. Figure 5 shows the most extensive sampling transect at x = 50 cm.

The multi-point samplers were designed to allow for measurement of both liquid and vapor phases. The samplers were constructed using 1.3 mm I.D. stainless steel chromatography tubing cut to specific sampling lengths (ranging from 5 to 45 cm). The sampling tubes were joined using a lead free tin solder with an all-purpose soldering flux. The samplers were inserted horizontally through the back wall of the flow system and sealed in place using a stainless steel sheath and Swagelock® compression fitting. The extraction ends of the samplers were completed with Teflon syringe sampling ports. The multi-point samplers were constructed in 2-point, 3-point, 4-point, 5-point, and 10-point configurations. Figure 6 shows a 2-point sampler assembly.

<u>Placement of Porous Media and Multi-Point Samplers.</u> The porous media was emplaced dry in a series of 5-cm lifts to a final depth of 1 m. As each lift was completed the multi-point samplers were inserted horizontally and sealed in place. Once the sand and multi-point samplers were in place, water was slowly introduced into the system in a series of 10-cm stages. After the up-gradient head stabilized at each 10-cm increment, flow through the system was stopped and the head was allowed to stabilize for 12 hours before the next stage was introduced. This process was continued until an up-gradient head of 80 cm was established. Flow was then held constant through the system for a period of 7 days.

Table 1. Physical, hydraulic, and transport properties of the three-dimensional aquifer model.

Parameter	Value
Porous Media	Flint Silica #14
	(U.S. Silica, Ottawa, IL)
Porous Media Dimensions (length x width x height; m)	2.0 x 0.5 x 1.0
Median Grain Size (d_{50}; mm)	1.2
Porosity (n)	0.3
Longitudinal Dispersivity (α_L; m)	0.001 – 0.004
Transverse Dispersivity (α_T; m)	0.0002
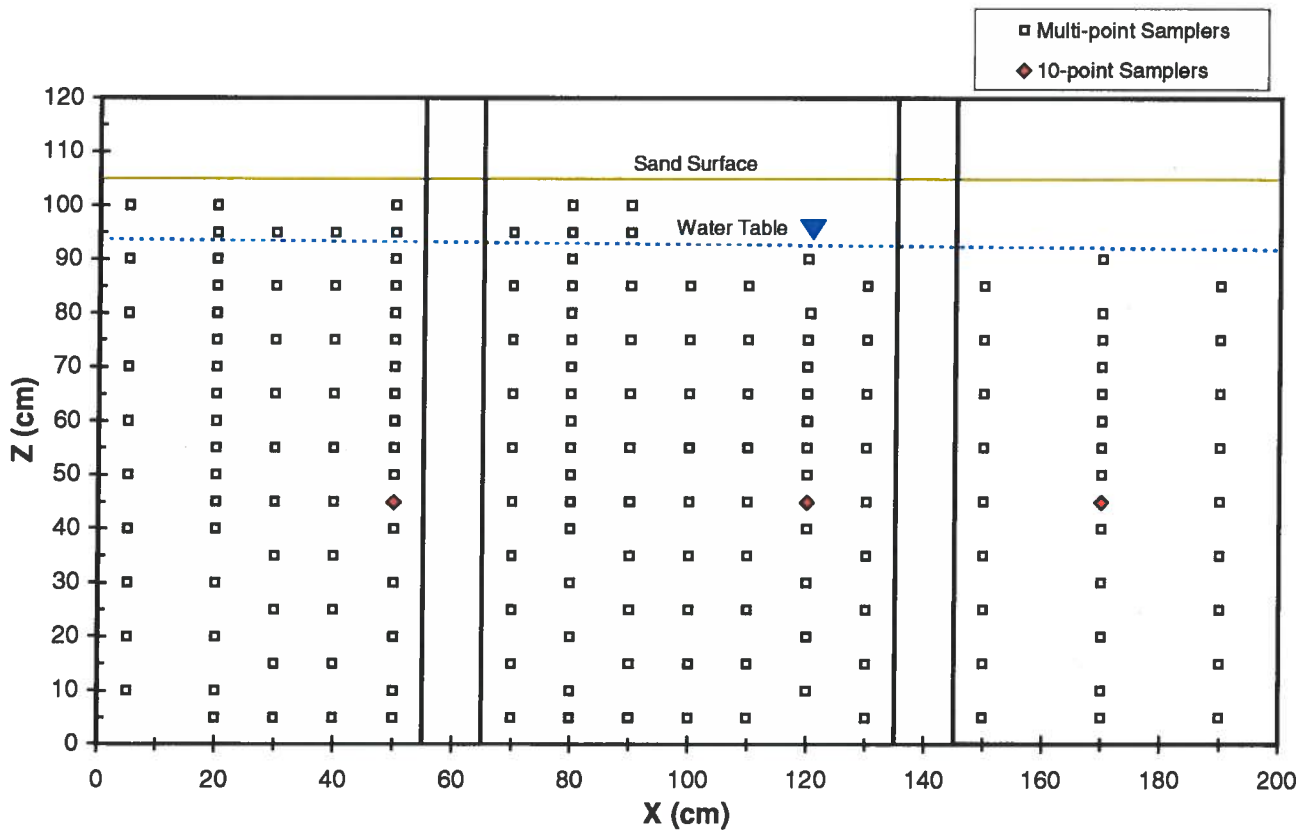
Figure 4. Schematic of the multi-sampler distribution along a longitudinal transect of the aquifer model.
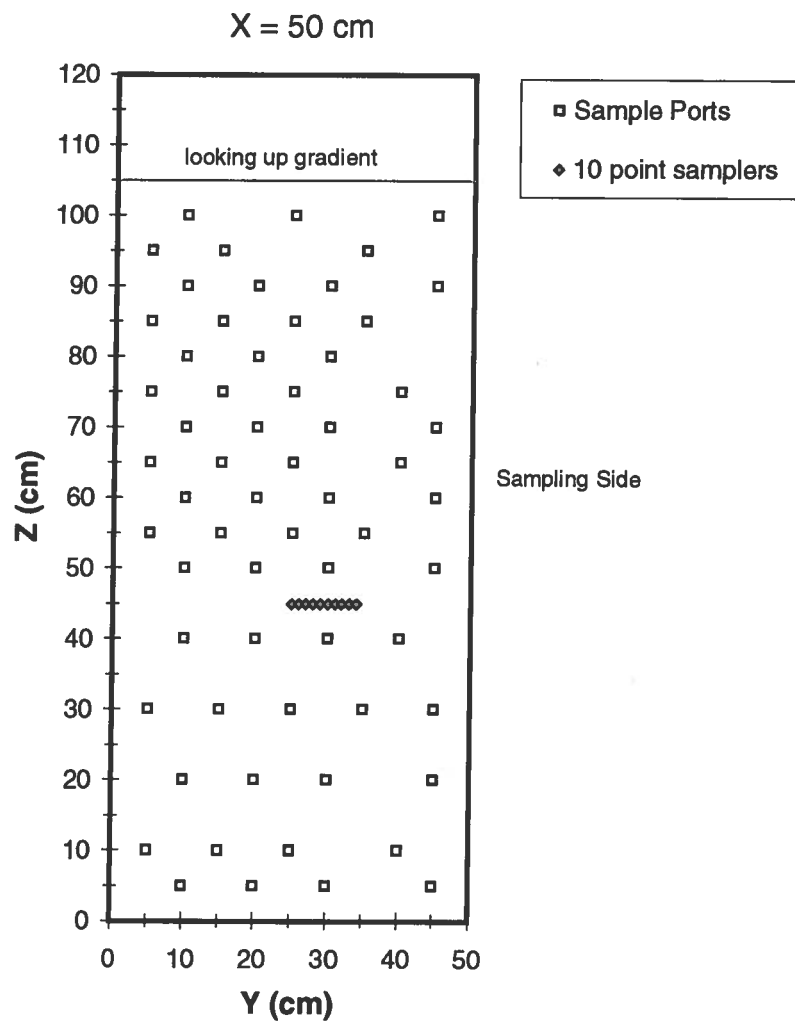
Figure 5. Schematic of the sample port distribution along a lateral transect (x = 50 cm) of the aquifer model.
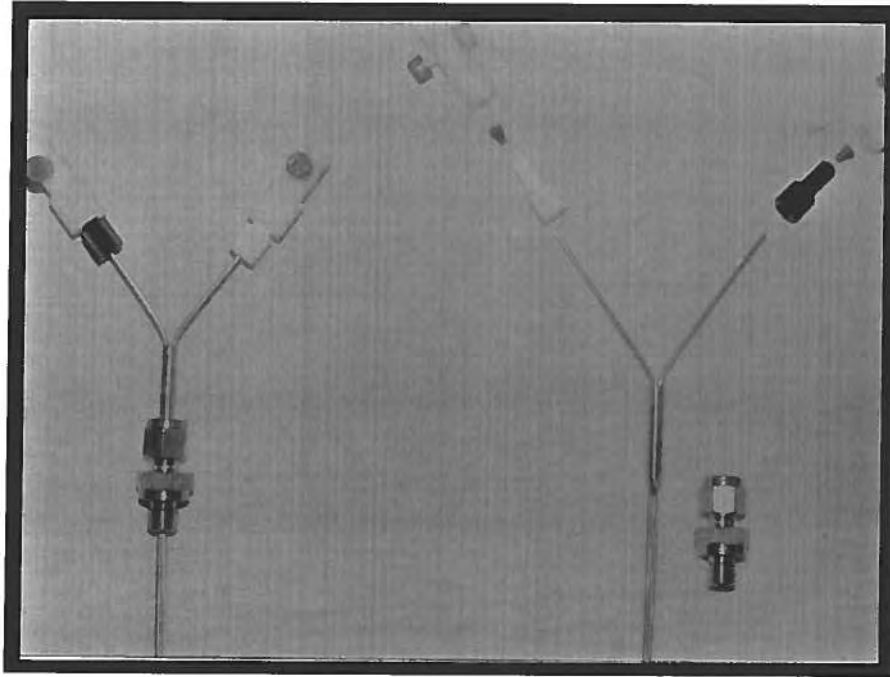
Figure 6. Two-point sampler assembly.

<u>Physical and Hydrodynamic Characterization of the System</u>. The porosity of the system was estimated by packing three columns with porous media and determining their dry mass (M_D). The columns were then saturated with water, and their saturated mass (M_S) was determined. An average value for porosity was computed as

$$n = \frac{M_w}{\rho_w V_T} \tag{1}$$

where n is the porosity of a given column, M_w is the water mass (M_S-M_D), V_T is the column volume, and ρ_w is the density of water (1.0 g/cm^3). The average porosity was determined to be 0.3.

Given that the model aquifer is of finite extent (2.0 m x 0.5 m x 1.0 m), application of the Dupuit assumptions (Bear 1979) for one-dimensional flow through a homogeneous unconfined aquifer allow for groundwater flow through the system to be estimated using a modified form of Darcy's Equation

$$Q_x = KWh_s \frac{(h_1 - h_2)}{L} \tag{2}$$

where Q_x [L^{3}T^{-1}] is the volumetric water discharge through the system, K [LT^{-1}] is the hydraulic conductivity, L and W are the length and width of the model aquifer; h_1 and h_2, are the up- and down-gradient head elevations; and h_s is the saturated and capillary fringe thickness at $L/2$ (Figure 7). Application of the Dupuit assumptions implies that all flow is horizontal, and in this case it is assumed that the water table is essentially linear. By assuming that the water table is linear between the up- and down-gradient heads (h_1 and h_2), the saturated thickness h_s can be estimated using the following relationship

$$h_s = \frac{h_1 + h_2}{2} + h_c \tag{3}$$

where h$_c$ is the capillary fringe thickness. Assuming uniform horizontal flow, and that the volumetric flowrate through the system (Q_x) can be approximated as the observed mean effluent flowrate, the bulk specific discharge q_x can be estimated as

$$q_x = \frac{Q_x}{Wh_s} \tag{4}$$

and the mean pore water velocity can be estimated as

$$v_x = \frac{Q_x}{nWh_s} \qquad (5)$$

where n is the system porosity.

If necessary, equation (2) can be used to estimate a bulk hydraulic conductivity value (K) for the system. However, it should be noted that because hydraulic conductivity is actually a constant of proportionality in equation (2), the estimated K value is specific to the current up- and down-gradient head values (h_1 and h_2) and corresponding saturated thickness (h_s).
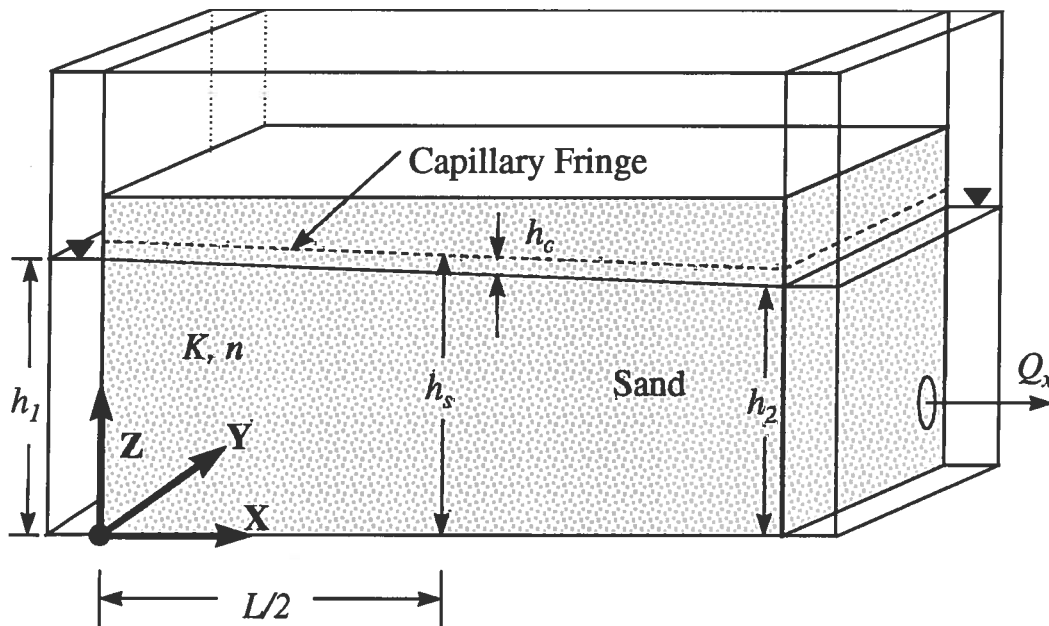

Figure 7: Steady unconfined flow through the three-dimensional aquifer model, assuming an essentially linear water table and one-dimensional horizontal flow in the x-direction.

EXPERIMENTS

Transport Characterization. In order to determine the longitudinal and transverse dispersivities (α_L and α_T) of the model aquifer, an ionic tracer experiment was performed. The experimental conditions and parameters are summarized in Table 2 and a conceptual diagram is shown in Figure 8. First, a steady flow field was established with an average saturated thickness (h_s) of 0.969 m, and an average pore water velocity of 0.42 m/day. Then a 20-mg/L solution of non-reactive chloride (Cl^-) tracer was injected from a continuous point source located near the inlet boundary at the center of the flow field (x = 0.025 m, y = 0.25 m, and z = 0.45 m). Transient, chloride concentrations were measured at three locations (x = 0.5 m, x = 1.2 m, and x = 1.7 m) along the centerline of the plume (Figure 9). Once the plume reached steady state, transverse (horizontal) concentration distributions were measured at the same x-locations, on three consecutive days (Figure 10).

The transverse concentration distributions were measured using 10-point samplers that were designed specifically for this experiment. The 10-point samplers were constructed and installed in order to provide a distribution of sample points with a 1-cm interval ranging from the centerline to the lateral extent of the plume. This allowed for the measurement of steady state transverse concentration profiles within the plume as shown in Figure 10. Assuming that the plume was symmetric (implying that the vertical and horizontal transverse dispersion was the same), the observed concentration distributions were used to estimate the transverse dispersivity within the system.

Table 2. System parameters for the transport characterization experiment.

Parameter	Value
Chloride Source	
Location (x, y, z; m)	.025, 0.50, 0.45
Concentration (mg/L)	20
Injection Rate (Q_s; m^3/day)	5.774×10^{-4}
Saturated Thickness at L/2 (h_s; m)	0.969
Average Effluent Water Flowrate (Q_x; m^3/day)	0.061
Average Pore Water Velocity (v; m/day)	0.42

Transient breakthrough curves (Figure 8)

Steady-state transverse concentration distributions (Figure 9)
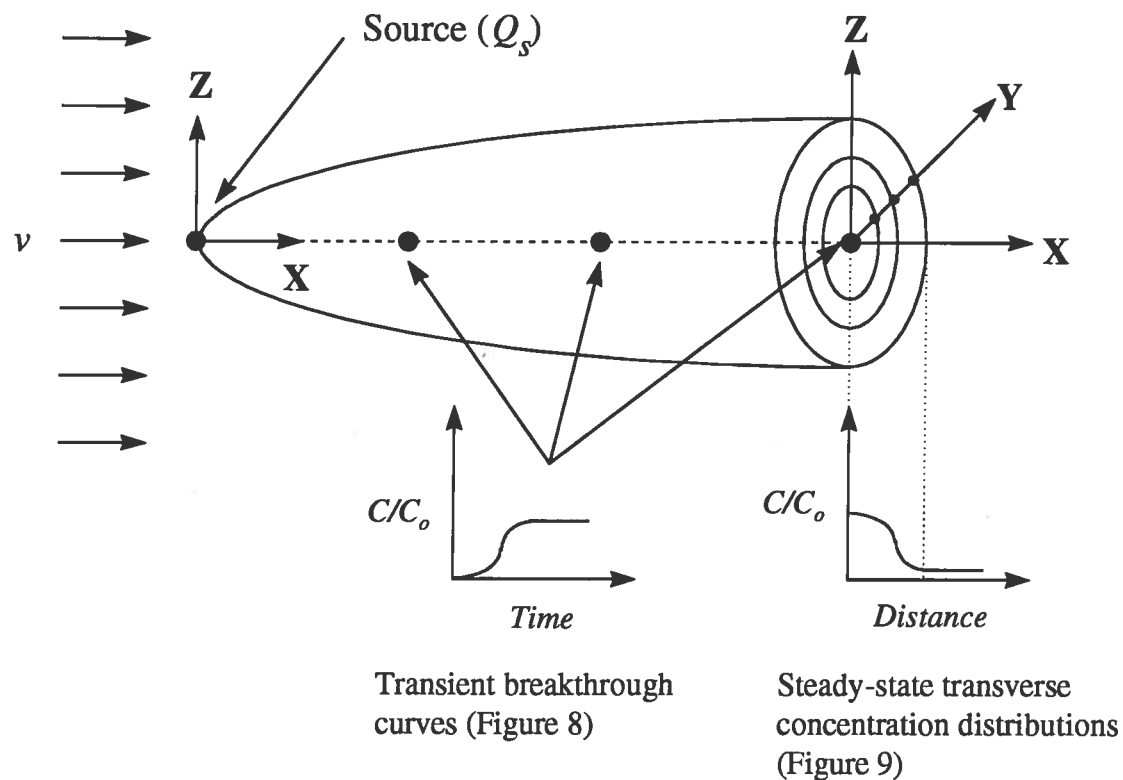
Figure 8. Conceptual diagram of transport characterization experiment performed to estimate longitudinal and transverse dispersivities.
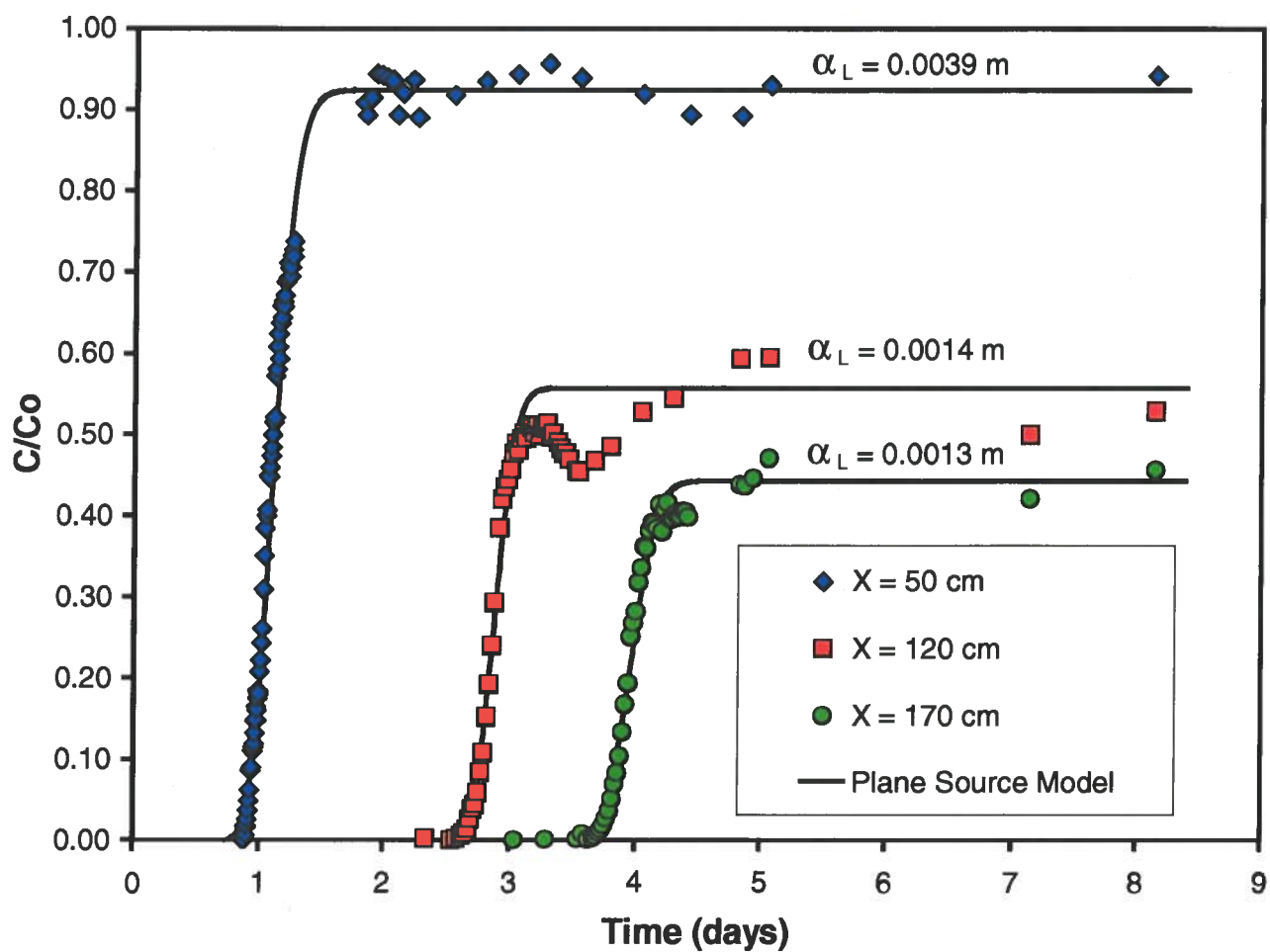
Figure 9. Chloride breakthrough curves (x = 50, 120, and 170 cm) and the corresponding longitudinal dispersivity values determined using a Levenberg-Marquardt nonlinear parameter estimation routine.

13
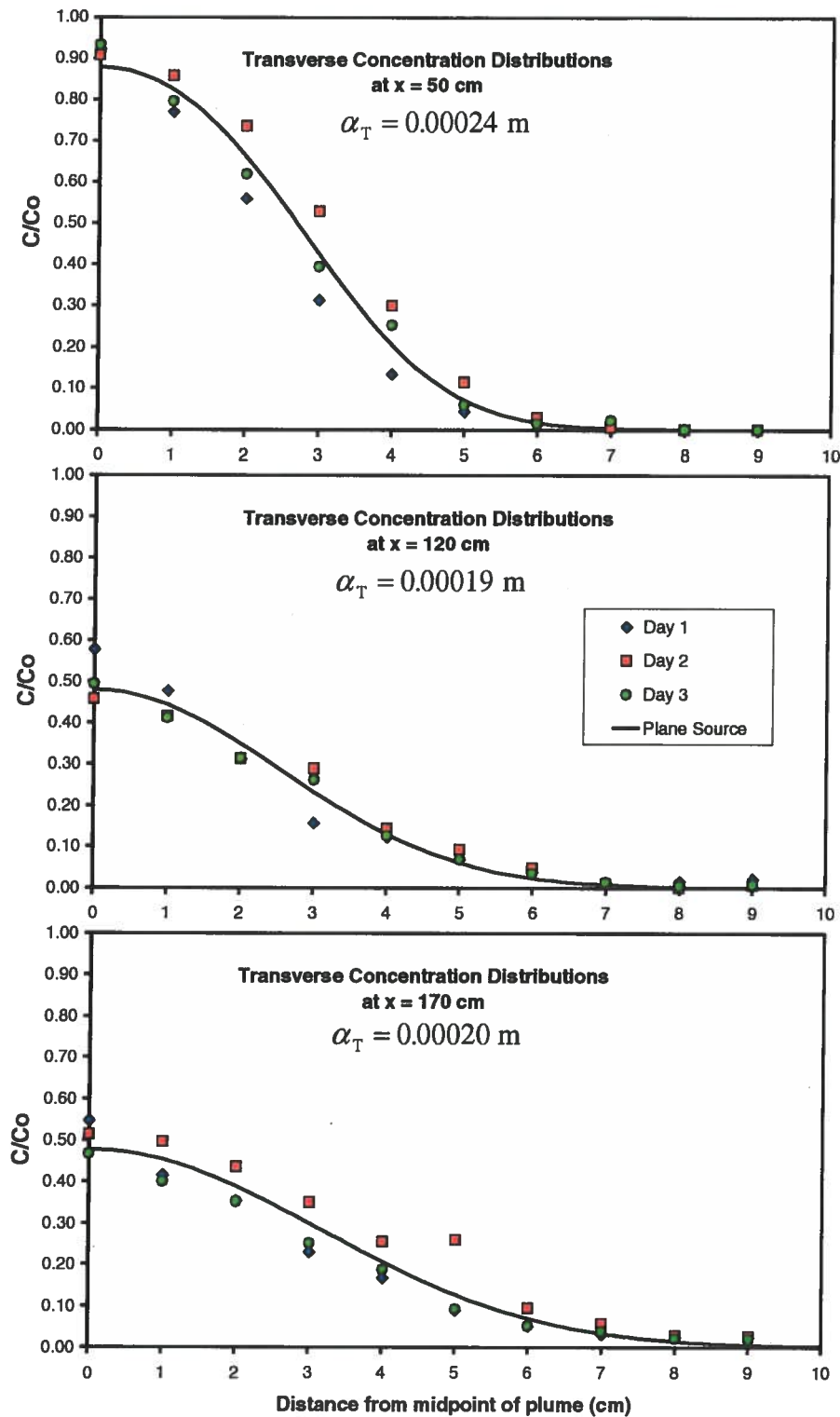
Figure 10. Transverse chloride concentration distributions and corresponding transverse dispersivity values determined using a Levenberg-Marquardt nonlinear parameter estimation routine.

14

The curves fit to the data in Figures 9 and 10 and the resulting dispersivity values were obtained using a Levenberg-Marquardt nonlinear parameter estimation algorithm (Marquardt 1963) and the analytical solution for three-dimensional transport from a continuous plane source (Domenico and Robbins 1985), rewritten in terms of the normalized concentration $\frac{C}{C_o}$ and by assuming that the horizontal and vertical transverse dispersivities are equal ($\alpha_y = \alpha_z = \alpha_T$).

(6)

$$\frac{C}{C_o} = \frac{1}{8} erfc\left[\frac{x-vt}{2(\alpha_L vt)}\right]\left\{erf\left[\frac{y+b}{2(\alpha_T x)^{1/2}}\right] - erf\left[\frac{y-b}{2(\alpha_T x)^{1/2}}\right]\right\}\left\{erf\left[\frac{z+d}{2(\alpha_T x)^{1/2}}\right] - erf\left[\frac{z-d}{2(\alpha_T x)^{1/2}}\right]\right\}$$

where C is the plume concentration at location x, y, z and C_o is the source concentration. The dimensions b and d represent the half-width and half-height of the plane source, v is the pore water velocity, α_L and α_T are the longitudinal and transverse dispersivities, and t represents the elapsed time. Under steady state conditions

$$\text{As } t \to \infty; \quad \frac{x-vt}{2(\alpha_x vt)^{1/2}} \to -\infty; \quad erfc(-\infty) \to 2 \tag{7}$$

equation (6) reduces to

$$\frac{C}{C_o} = \frac{1}{4}\left\{erf\left[\frac{y+b}{2(\alpha_T x)^{1/2}}\right] - erf\left[\frac{y-b}{2(\alpha_T x)^{1/2}}\right]\right\}\left\{erf\left[\frac{z+d}{2(\alpha_T x)^{1/2}}\right] - erf\left[\frac{z-d}{2(\alpha_T x)^{1/2}}\right]\right\} \tag{8}$$

In order to apply equations 6 and 8 the source dimensions b and d were estimated by equating the specific discharge of the source (q_s) to the specific discharge of the system (q_x). Knowing that the specific discharge is defined as the volumetric flowrate through a given cross-sectional area, and assuming a square plane source ($b = d$) the source dimension can be estimated as

$$b = \left[\frac{Wh_s}{4} \left(\frac{Q_s}{Q_x} \right) \right]^{1/2} \tag{9}$$

where W is the width of the model aquifer, h_s is the average saturated thickness, Q_s is the source

injection rate, and Q_x is the mean flowrate through the system.

With an estimate for the source dimensions b and d; equation 8 was used with the

Levenberg-Marquardt parameter estimation algorithm to determine the transverse dispersivities

(α_T) corresponding to each transverse concentration distribution (Figure 10). The estimated

values of α_T were then used with equation (6) and the Levenberg-Marquardt algorithm to

estimate the longitudinal dispersivities (α_L) corresponding to each transient breakthrough curve

(Figure 9). The average transverse dispersivity for the three observation locations (x = 50 cm, x

= 120 cm, and x = 170 cm) was 0.0002 m, as listed in Table 1. It can be seen in Figure 9 that the

longitudinal dispersivity value estimated at x = 50 cm (0.0039 m) is slightly higher than the

values at x = 120 cm and x = 170 cm (0.0014 m and 0.0013 m respectively). Inspection of the

breakthrough curve at location x = 50 cm reveals that the transition between the transient (rising

limb) and steady state (plateau) portions of the curve was not accurately captured. It is believed

that this missing information may have lead to the slightly higher longitudinal dispersivity

estimate. But, rather than ignore a portion of the data set, it was decided to report the

longitudinal dispersivity as a range of values (0.001 m to 0.004 m) as listed in Table 1.

When estimating the dispersivities, the analytical solution for transport from a continuous

plane source was used rather than a solution for a continuous point source in order to provide

agreement with the mathematical model presented in Newman (2000). Dispersivities estimated

using a point source solution would be greater than those estimated using the plane source

solution. This is because the plane source represents a larger source area than a discrete point.

16

Tracer traveling from a point source would have to disperse a greater lateral distance in order to reach the same transverse location as tracer traveling from the extent of a plane source.

Multiple Ionic Tracer Experiments. Once the physical, hydrodynamic, and transport characteristics of the aquifer model had been established, experiments were preformed to provide a sequential set of data to test the capabilities of the mathematical model and numerical solution techniques presented in Newman (2000). The first experiment was a multiple source ionic tracer experiment and the second was a multiple source DNAPL dissolution experiment.

The multiple source ionic tracer experiment was started by establishing a steady flow field with an average saturated thickness (h_s) of 0.94 m, and an average pore water velocity of 0.45 m/day. Then, three steady state plumes were developed by continuous injection of bromide (Br^-), chloride (Cl^-), and sulfate (SO_4^{-2}) tracer solutions (200 mg/L each) from three separate injection ports, located within the up-gradient saturated region of the flow system. Experimental conditions and parameters are summarized in Table 3 and the source locations are shown in Figure 11.

Table 3. System parameters for the multi-source ionic tracer experiment.

| Parameter	Value
Source No. 1 (Chloride)	
Injection Point Location (x, y, z; m)	0.20, 0.25, 0.65
Concentration (mg/L)	200
Injection Rate (mL/hour)	1.152×10^{-3}
Source No. 2 (Bromide)	
Injection Point Location (x, y, z; m)	0.20, 0.20, 0.50
Concentration (mg/L)	200
Injection Rate (mL/hour)	5.76×10^{-4}
Source No. 3 (Sulfate)	
Injection Point Location (x, y, z; m)	0.20, 0.30, 0.50
Concentration (mg/L)	200
Injection Rate (mL/hour)	5.76×10^{-4}
Saturated Thickness at L/2 (h_s; m)	0.94
Average Effluent Water Flowrate (Q_x; m^3/day)	0.0635
Specific Discharge (q_x, m/day)	0.135
Average Pore Water Velocity (v; m/day)	0.45
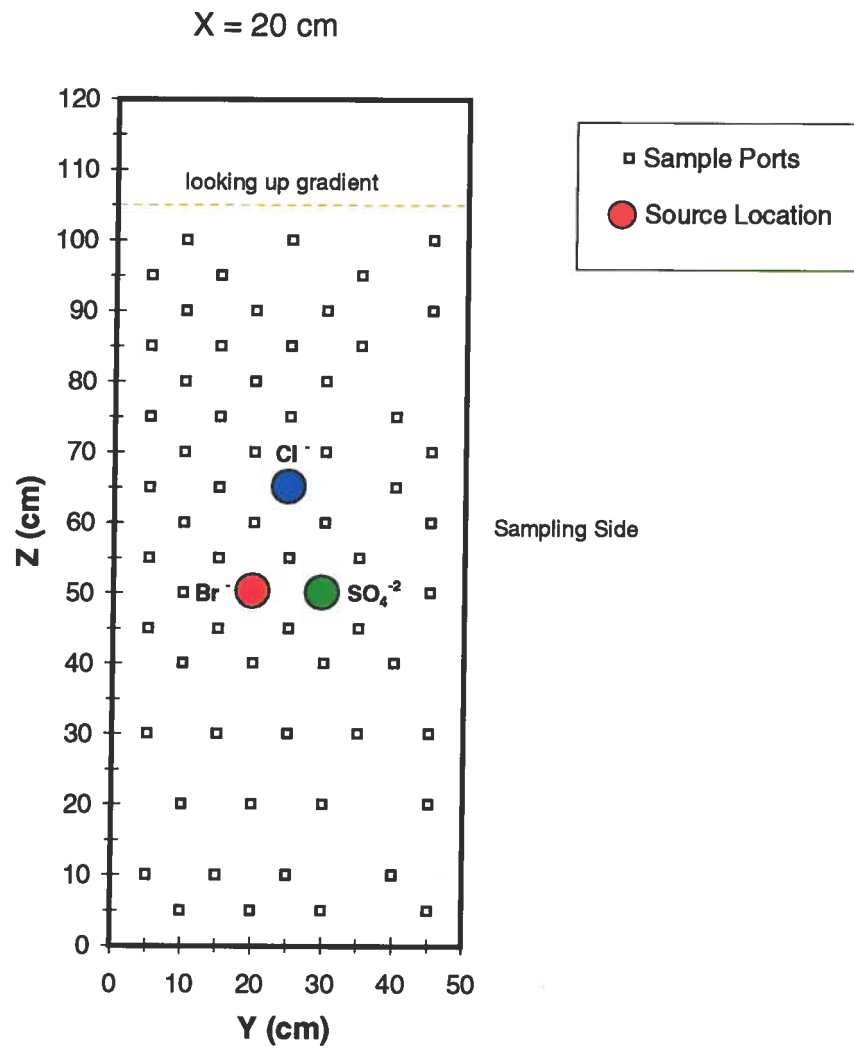
Figure 11. Source locations (transect x = 20 cm) for multiple source ionic tracer experiment.

Transient tracer concentrations were measured at multiple locations along the flow path in order to determine when steady state conditions were established. Once the plumes had reached steady state (day 6), tracer concentrations were collected throughout the entire model aquifer domain on two consecutive days (day 7 and day 8). These data provided two "snap shots" of the steady state tracer distribution within the porous media and are shown in Figures 12 and 13. Inspection of Figures 12 and 13 provides a good indication that steady state conditions were established, as the plume extents and concentration magnitudes are practically identical.

The reason for using three different ionic tracers was to provide the ability to distinguish between the contributions of each point source to the combined downgradient plume. For modeling purposes the tracer concentrations can be combined and treated as one single contaminant, but having the ability to distinguish between the contributions of each source allowed for additional scrutiny of each of the numerical models capabilities to estimate the spatial distribution of mass flux. It also provided helpful information for trouble-shooting simulated flux values at zones of plume overlap during the early stages of model verification.

Multiple Source DNAPL Dissolution Experiment. The multiple source DNAPL experiment was started by establishing a steady flow field with an average saturated thickness (h_s) of 0.922 m, and an average pore water velocity of 0.34 m/day. Once steady flow was established, ten DNAPL sources, composed of a mixture of 55% n-hexadecane and 45% perchloroethene (PCE) by volume, were emplaced within the up-gradient region of the flow system by slow injection of a known volume (approximately 10 ml for each source). The corresponding mole fractions were 0.3 for n-hexadecane and 0.7 for PCE. The NAPL solution also contained the hydrophobic dye oil red-o. Experimental conditions and parameters are summarized in Table 4-4 and the source locations are shown in Figures 14 and 15.
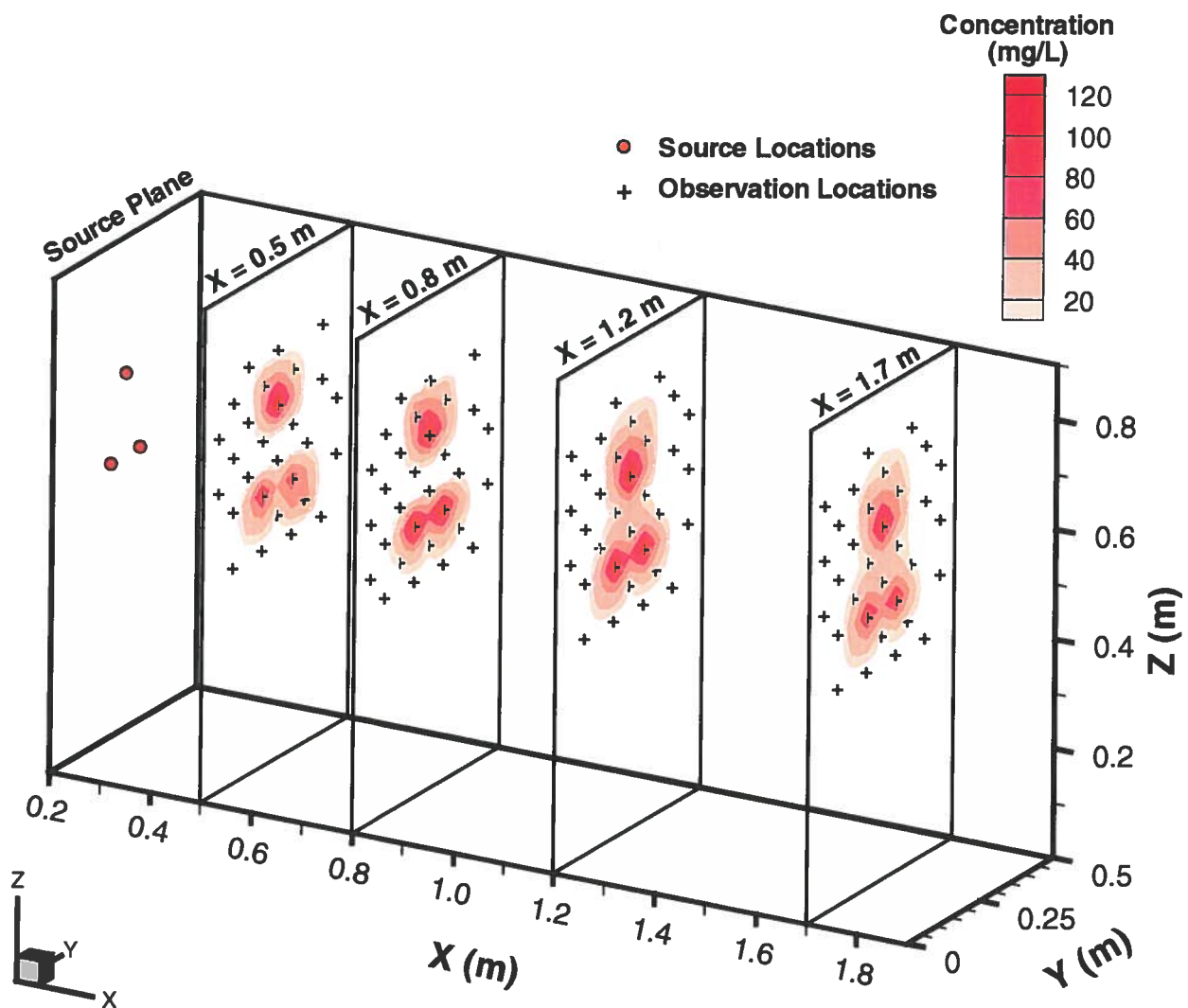
20

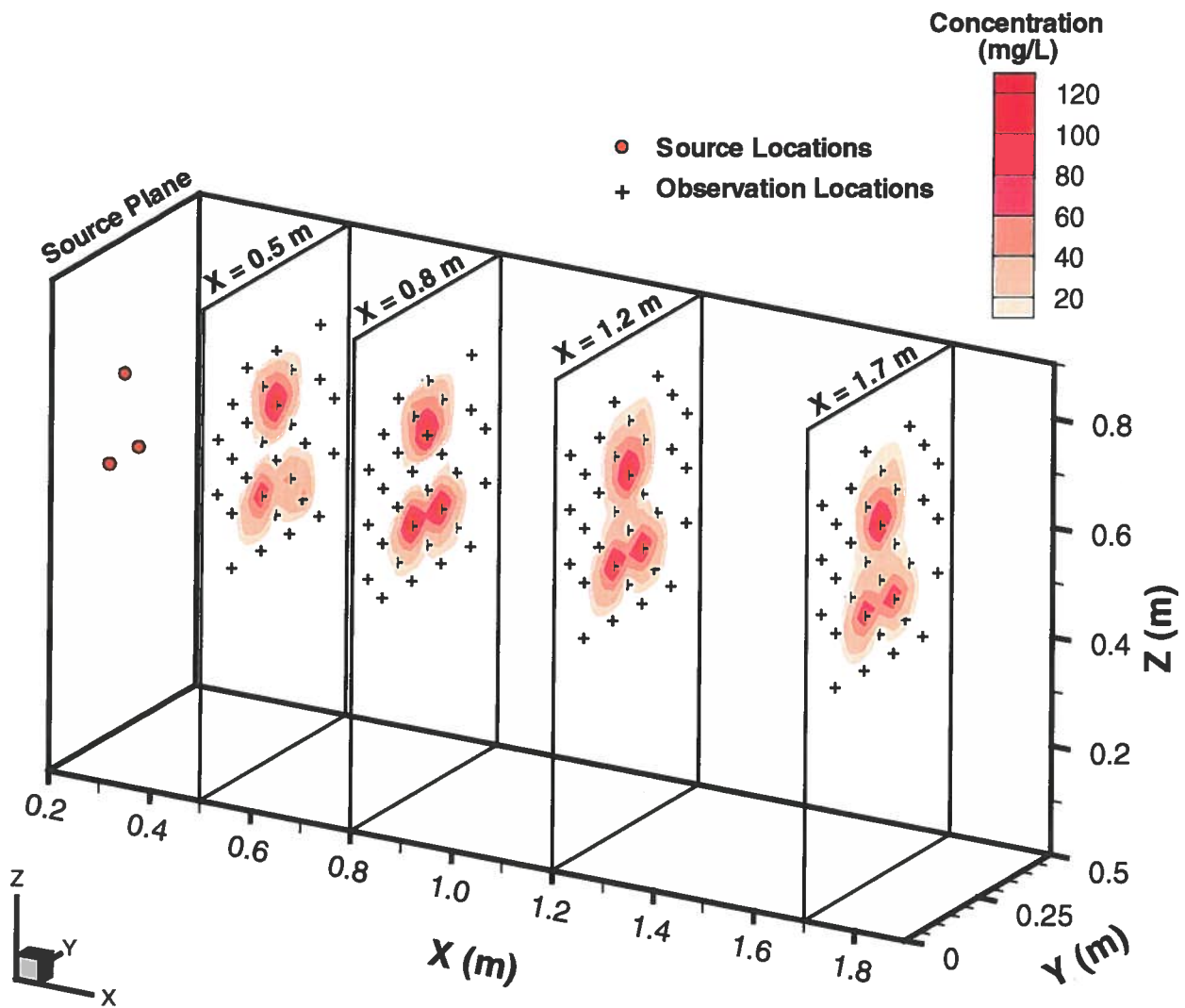Figure 12. Steady state three-dimensional ionic tracer plume distribution for Day 7.

Figure 13. Steady state three-dimensional ionic tracer plume distribution for Day 8.
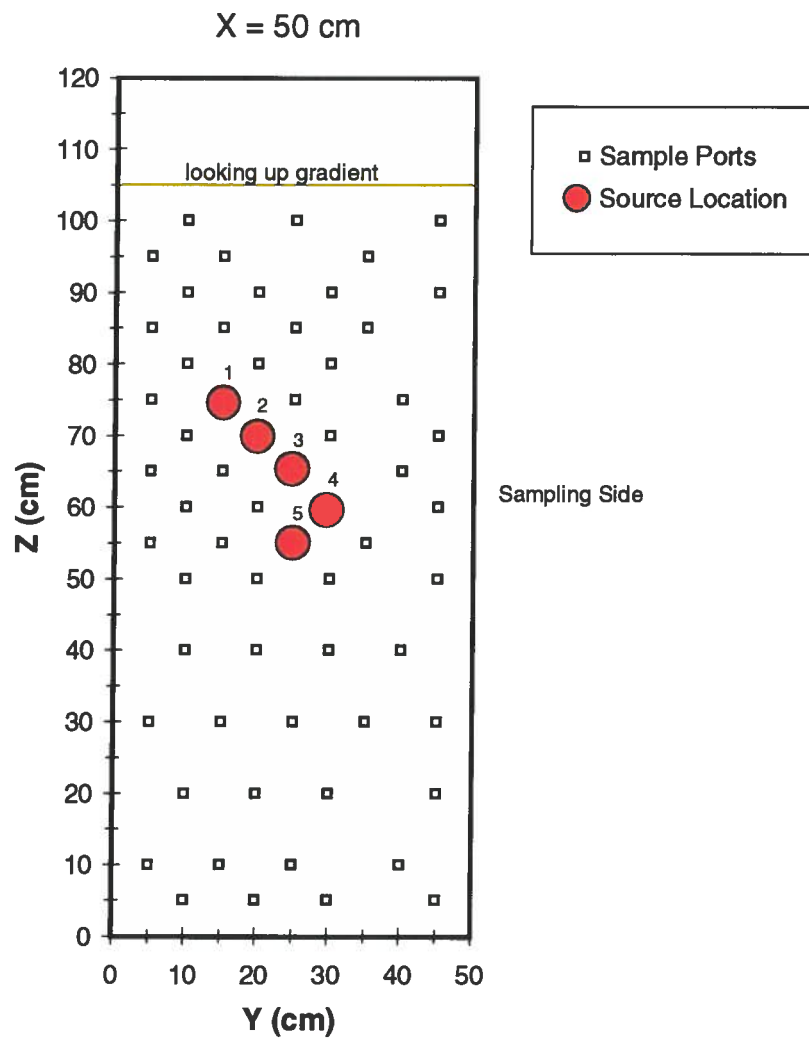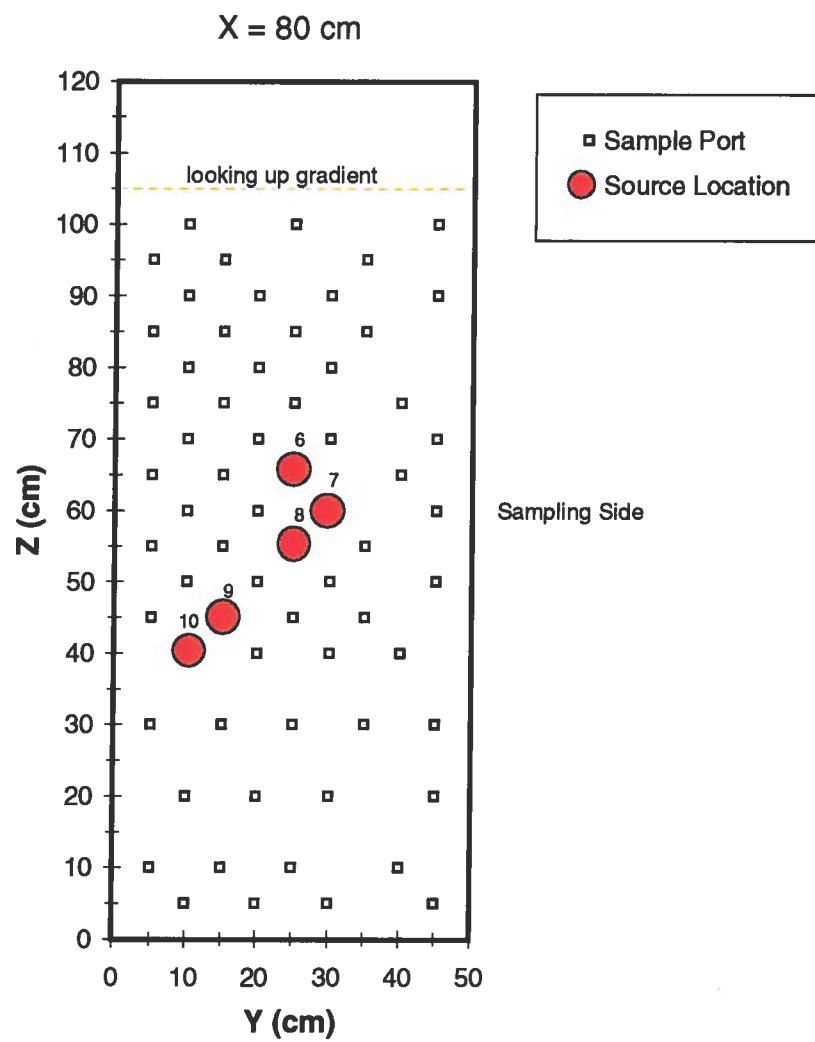
Figure 14. DNAPL source locations at transect x = 50 cm.

Figure 15. DNAPL source locations at transect x = 80 cm.

The n-hexadecane was included in the NAPL solution for the following two reasons: to prolong the life of the PCE source zones and to help provide a visual indicator of the source zone distribution that could be recorded during excavation of the system. N-hexadecane is a hydrophobic compound, which means that it has an extremely low aqueous solubility ($S_{n\text{-}hexa}$ = 3.588×10^{-3} mg/l). By including an extremely hydrophobic compound in the NAPL mixture, a partitioning media for the PCE was created which acts to reduce the effective solubility of PCE. Reducing the effective solubility of PCE increases the lifetime of the PCE source zones. This concept can be illustrated through the use of an analog of Raoult's Law for the vapor pressure of a solution. Raoult's law states that *the vapor pressure of a solution component above a solution is equal to the product of the vapor pressure of the liquid and its mole fraction in solution* (Petrucci, 1985). The aqueous analog of this relationship can be expressed as

$$S^e_{i(w)} = X_{i(N)} S^o_{i(w)} \tag{10}$$

where $X_{i(N)}$ is the mole fraction of component i in the NAPL mixture, $S_{i(w)}$ is the pure aqueous solubility of NAPL component i, and $S^e_{i(w)}$ is the resulting effective aqueous solubility of component i.

Pankow and Cherry (1996) observed that there was a wide range of aqueous solubility limits reported in the literature for chlorinated solvents such as PCE and TCE. A review of the literature found that the aqueous solubility of PCE is reported to range between 149 mg/l (Lesage and Brown, 1993) and 200 mg/L (Mabey et. al, 1982). Knowing that the NAPL source solution was composed of 45% PCE and 55% n-hexadecane by volume, and using the range of reported PCE solubility limits, equation (10) can be used to estimate the expected experimental range of effective solubility for PCE. The result is that the maximum expected aqueous phase PCE

concentration during the NAPL dissolution experiment should be within the range 105 to 140 mg/L. Thus, by using n-hexadecane in the NAPL solution the solubility of PCE was reduced by 70 to 50% which decreased the rate at which PCE was removed from the system and lengthened the effective life of the experimental NAPL source zones.

The second benefit of including n-hexadecane was that because it is extremely hydrophobic, it would partition onto or coat the porous media. So, even as the source zones dissolve, a portion of n-hexadecane will remain on the soil—effectively marking the extent of the initial source zones. Because the dye, oil-red-o, is also hydrophobic it will partition preferentially into the n-hexadecane, thus providing a visual indication of the NAPL source zone spatial distribution. This was done so that during excavation the source zone distribution could be recorded.

The one drawback of using n-hexadecane was that it is a light nonaqueous phase liquid (LNAPL) meaning that its density ($\rho_{n-hexa} = 0.7733$ g/ml) is less than that of water ($\rho_w = 1.00$ g/ml). In order to assure that the NAPL solution would behave as a DNAPL the solution composition was selected such that the multi-component NAPL was denser than water ($\rho_{NAPL} = 1.16$ g/ml).

Aqueous phase PCE concentrations were collected from within the flow system during the transient stage of plume development, and over an extended time-period (approximately one month) in which the plume was essentially at steady state. Once the system had reached steady state, PCE concentrations were collected throughout the entire model aquifer domain on two occasions (day 44 and day 58). Figures 16 and 17 show the measured PCE concentration distributions. Inspection of the figures indicates that the PCE plume was essentially steady state, as the plume extents and the range of concentrations are similar.

Upon completion of the experiments the porous media was excavated and the source zone distribution indicated by oil red-o dye was recorded using an excavation grid and digital photographs (Figure 18). The extent of the DNAPL source zones in each photograph were manually digitized and combined to develop a three-dimensional representation of the DNAPL source zones (Figure 19). Knowing the three-dimensional spatial distribution of the DNAPL sources provided an accurate assessment of the ability of the mathematical models (Newman, 2000) to determine the spatial distribution of contaminant mass flux values within a zone of multiple sources.

Table 4. System parameters for the multi-source DNAPL experiment.

| Parameter	Value
Source No. 1	
Injection Point Location (x, y, z; m)	0.50, 0.15, 0.75
Volume Delivered (mL)	10.78
Source No. 2	
Injection Point Location (x, y, z; m)	0.50, 0.20, 0.70
Volume Delivered (mL)	11.78
Source No. 3	
Injection Point Location (x, y, z; m)	0.50, 0.25, 0.65
Volume Delivered (mL)	10.45
Source No. 4	
Injection Point Location (x, y, z; m)	0.50, 0.30, 0.60
Volume Delivered (mL)	10.44
Source No. 5	
Injection Point Location (x, y, z; m)	0.50, 0.25, 0.55
Volume Delivered (mL)	10.15
Source No. 6	
Injection Point Location (x, y, z; m)	0.80, 0.25, 0.65
Volume Delivered (mL)	10.44
Source No. 7	
Injection Point Location (x, y, z; m)	0.80, 0.30, 0.60
Volume Delivered (mL)	10.44
Source No. 8	
Injection Point Location (x, y, z; m)	0.80, 0.25, 0.55
Volume Delivered (mL)	10.44
Source No. 9	
Injection Point Location (x, y, z; m)	0.80, 0.15, 0.45
Volume Delivered (mL)	10.44
Source No. 10	
Injection Point Location (x, y, z; m)	0.80, 0.10, 0.40
Volume Delivered (mL)	10.44
Saturated Thickness at L/2 (h_s; m)	0.922
Average Effluent Water Flowrate (Q_x; m^3/day)	0.047
Specific Discharge (q_x, m/day)	0.102
Average Pore Water Velocity (v; m/day)	0.34
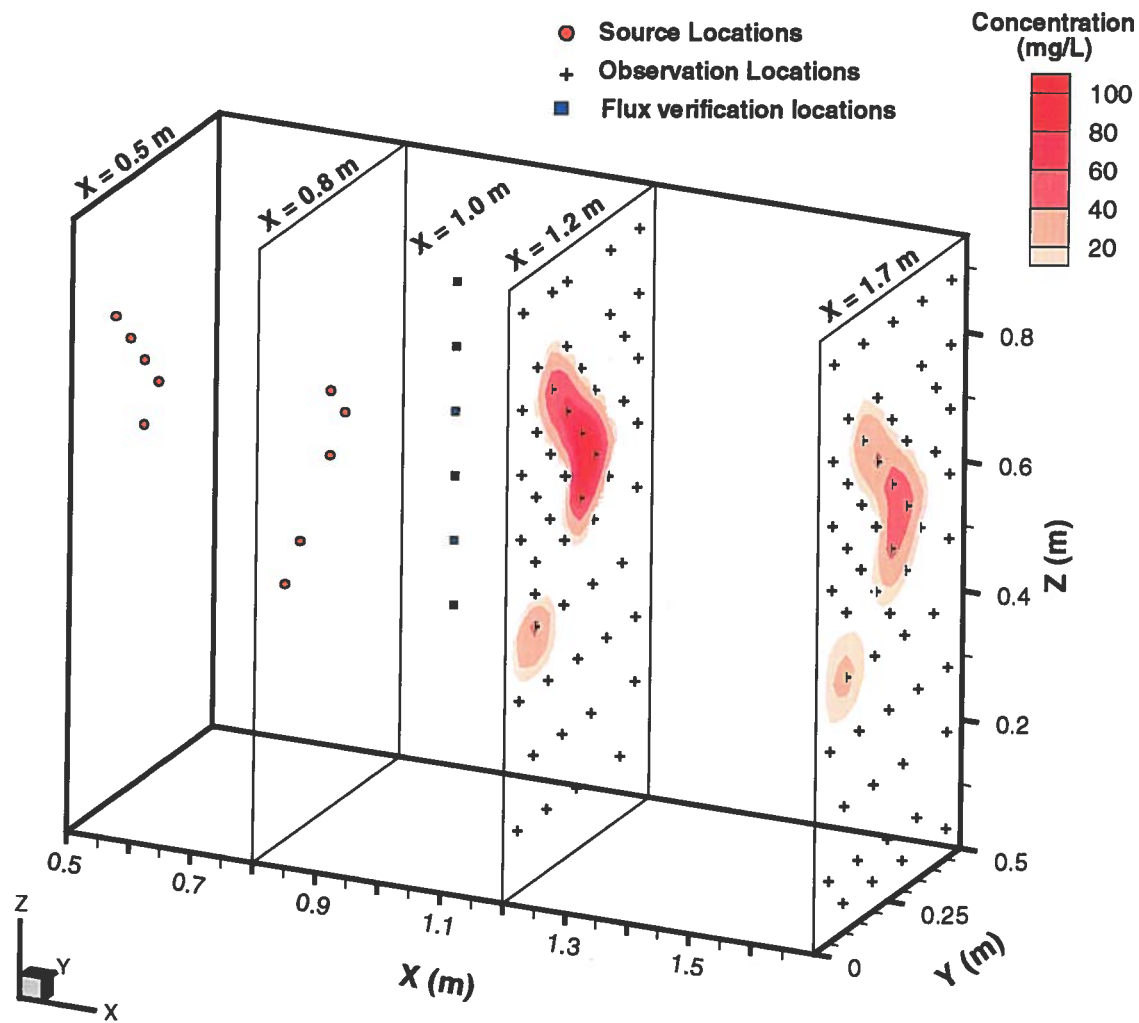
Figure 16. Steady state three-dimensional PCE concentration distribution for Day 44.
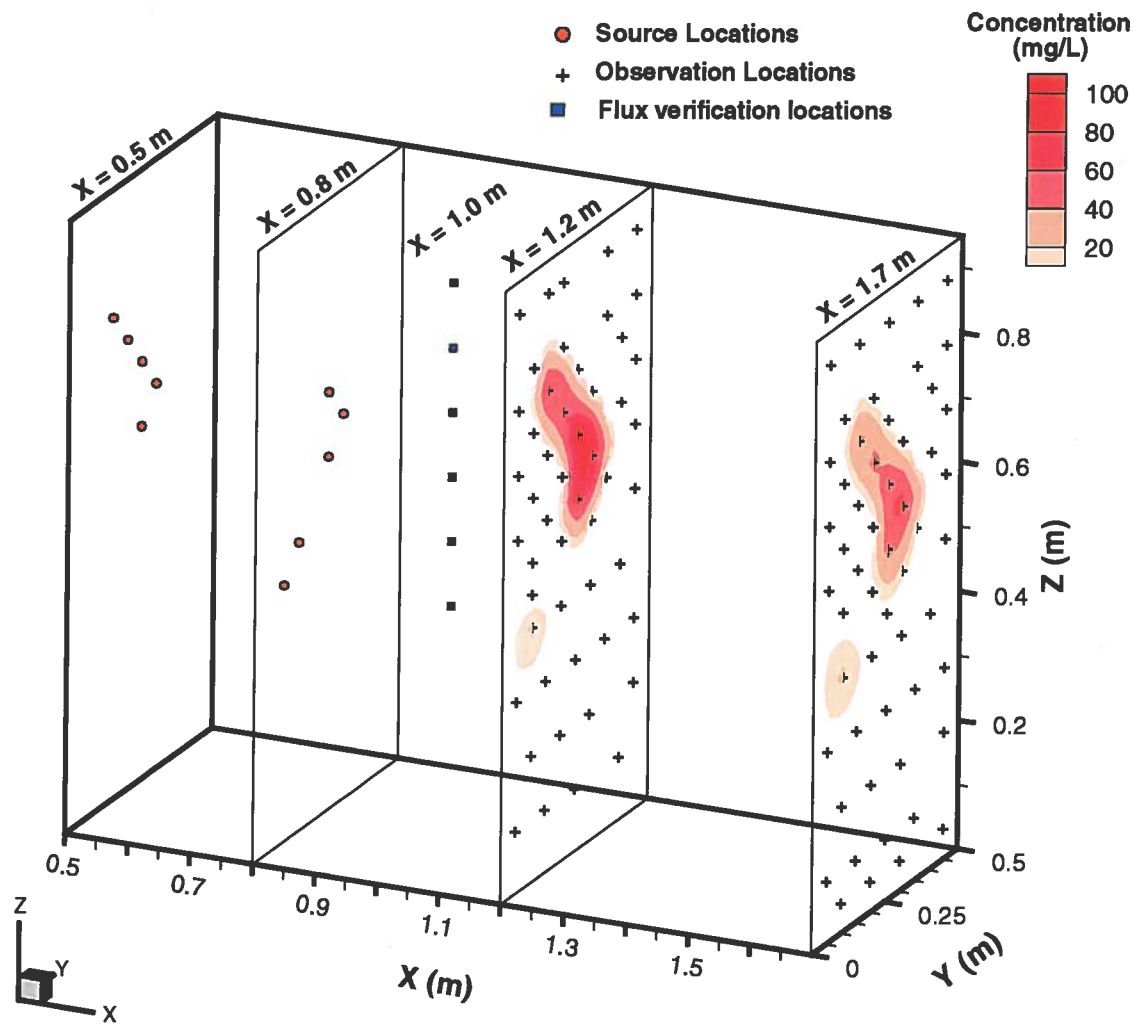
Figure 17. Steady state three-dimensional PCE concentration distribution for Day 58.
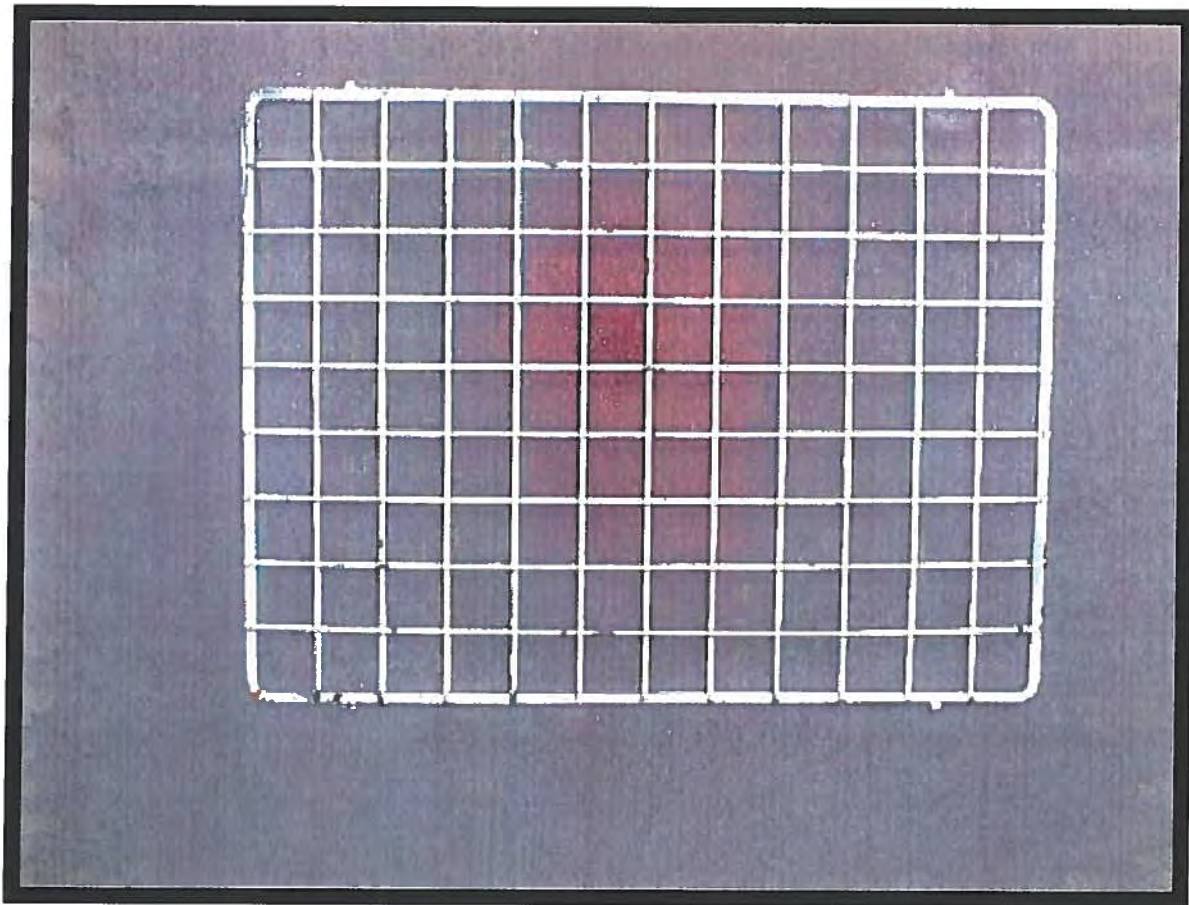
Figure 18. An excavation photograph showing the excavation grid (2 cm x 2 cm grid cells) and a portion of the DNAPL source zone.
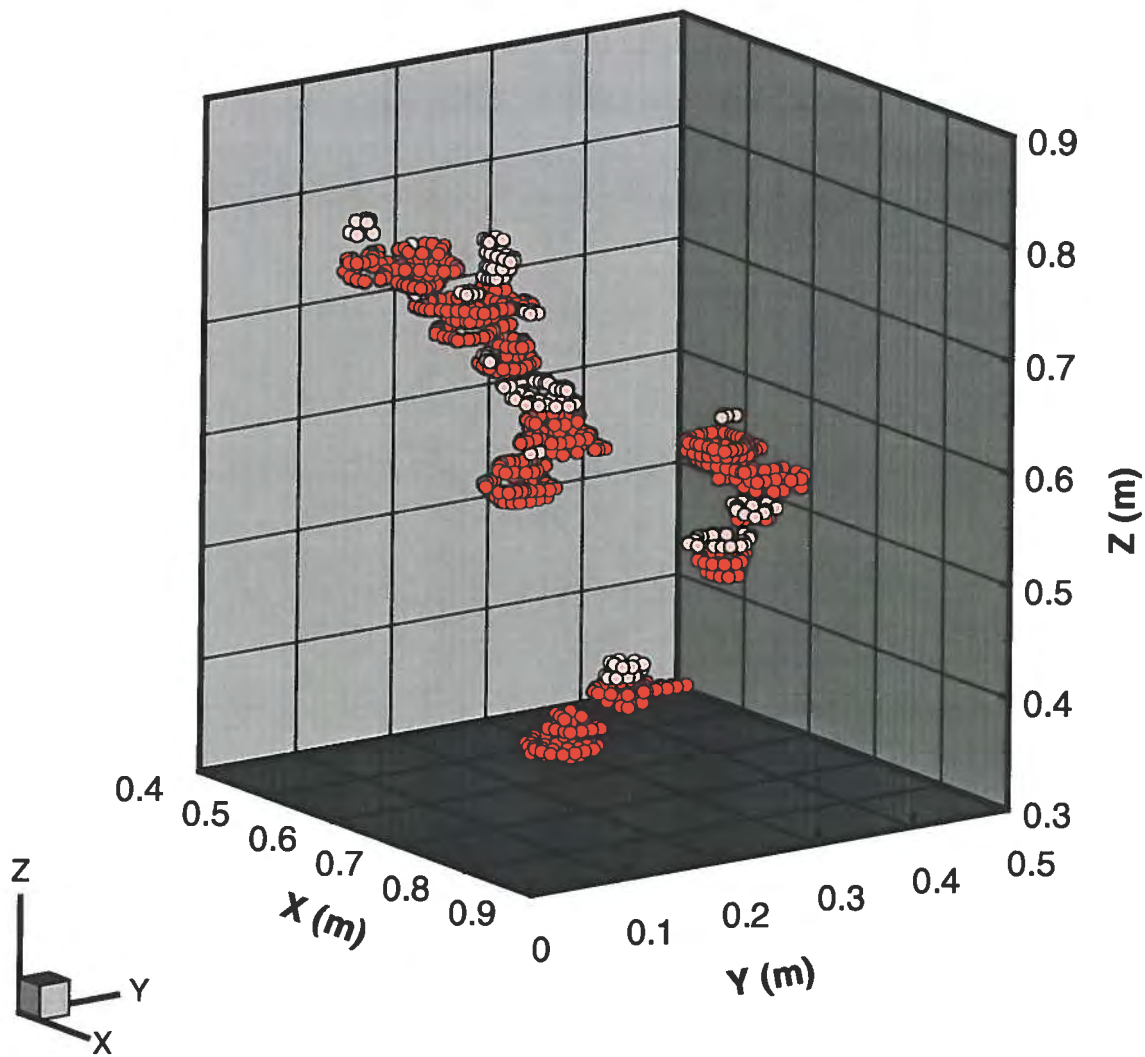
Figure 19. Three-dimensional representation of DNAPL source zone based upon digital excavation photographs. (The color shown matches the observed dye intensity in the excavation photographs).

SUMMARY

The physical modeling study described in this report successfully met many of the objectives originally conceived for the project. Unfortunately, program changes and funding redirection resulted in the project being halted before all objectives could be met. During the study, a unique physical modeling system was designed and constructed to examine the dissolution behavior of chlorinated solvents in porous aquifers under dynamic flow conditions. The physical modeling system allowed quantitative mass balance to be achieved for chlorinated solvent mass in groundwater, vapor, and solid phases within the model domain. Although designed to simulate homogeneous and non-homogeneous phreatic aquifers, experiments performed during this study only used the homogeneous configuration. Several experiments were performed to characterize the hydraulics and hydrodynamics of the physical model, and to examine the behavior of co-mingled plumes emanating from multiple ionic source zones. These experiments were followed by multi-source DNAPL dissolution experiments. Results form these experiments were used by Newman (2001) to develop and test inverse numerical modeling methods for locating DNAPL source zones with minimal concentration measurement data. The numerical tools developed using quantitative data gathered during this study demonstrate the usefulness and importance of multi-dimensional physical modeling experimental techniques.

REFERENCES

Annable, M.D., Jawitz, J.W., Rao, P.S.C., Dai, D.P., Kim, H. and Wood, A.L. (1998a). Field evaluation of interfacial and partitioning tracers for characterization of effective NAPL-water contact areas. Ground Water 36(3): 495-502.

Annable, M.D., Rao, P.S.C., Hatfield, K., Graham, W.D., Wood, A.L. and Enfield, C.G. (1998b). Partitioning tracers for measuring residual NAPL: field-scale test results. Journal of Environmental Engineering 124(6): 498-503.

Bear, J. (1979). Hydraulics of groundwater. New York, McGraw-Hill, Inc.

Domenico, P.A. and Robbins, G.A. (1985). A new method of contaminant plume analysis. Ground Water 23(4): 476-485.

Jin, M., Delshad, M., Dwarakanath, V., McKinney, D.C., Pope, G.A., Sepehrnoori, K., et al., (1995). Partitioning tracer test for detection, estimation, and remediation performance assessment of subsurface nonaqueos phase liquids. Water Resources Research 31(5): 1201-1211.

Lesage, S. and Brown, S. (1994) Observation of the dissolution of NAPL mixtures. Journal of Contaminant Hydrology, 15: 57-71.

Mabey, W.R., Smith, J.H., Podoll, R.T., Johnson, H.L., Mill, T., et al., (1982) Aquatic fate process data for organic priority pollutants. United States Environmental Protection Agency, Washington DC. Report No. 440/4-81-014.

Marquardt, D.W. (1963). An algorithm for least-squares estimation of nonlinear parameters. J. Soc. Indust. Appl. Math. 11: 431-441.

Newman, M. A. Inverse Characterization of Subsurface Contaminant Mass Flux: A three-Dimensional Physical and Numerical Modeling Study, University of Florida, 2001.

Pankow, J.F. and Cherry, J.A. (1996). Dense Chlorinated Solvents and other DNAPLS in groundwater. Portland, Waterloo Press.